

Theory of the Saffman-Taylor "finger" pattern. II

David A. Kessler

Department of Physics, Rutgers University, Piscataway, New Jersey 08854

Herbert Levine

Schlumberger-Doll Research, Old Quarry Road, Ridgefield, Connecticut 06877-4108

(Received 5 September 1985)

We generalize the stability results of the preceding paper to arbitrary λ . Coupled with a new approach to the selection of "finger" width, this stability computation allows us to predict the dependence of allowed widths on capillary number. At the same time, we show that of all possible finger shapes at fixed capillary number, only one [denoted $\lambda^*(\gamma)$] is stable. Finally, we show how finite noise can shift $\lambda^*(\gamma)$, causing observed widths and stability to diverge from the noiseless calculation at large velocity. We conclude with a discussion of the paradigm of microscopic solvability for diffusive controlled pattern formation, into which the above analysis neatly falls.

I. INTRODUCTION

In the preceding paper,¹ we studied the stability operator around the steady-state "finger" shape and concluded that all modes at $\lambda = \frac{1}{2}$ were damped in time. This calculation was carried out by deriving the steady-state shape to linear order in γ and then considering a perturbation, also to the same order. This is possible only because the selection of a discrete set of allowed finger shapes as demonstrated by McLean and Saffman² and Vanden-Broeck³ seems to be invisible in an asymptotic series in γ .

In this paper, we use the general λ version of the stability operator to study the true finger shape as a function of γ and its resultant stability. The first part is devoted to a reexamination of the paper of Vanden-Broeck. In particular, we use his method of determining the allowed set of λ at fixed γ to demonstrate that the selection mechanism is due to terms which are *essentially singular* as $\gamma \rightarrow 0$. This explains the inapplicability of asymptotic analysis as well as the results in paper I regarding the translation zero mode. Reversing the logic, we can then use the existence of a true zero mode as an indication of convergence of the asymptotic series. Using this, we reproduce the selected set to high accuracy.

The second part of this paper is devoted to the stability characteristics of the selected set. By virtue of the selection mechanism, it turns out that it is inevitable that all but the largest velocity (smallest λ) member of the discrete set [$\lambda^*(\gamma)$] will be unstable. This explains the agreement of the experiments with λ^* . We study the continuum around λ^* as well as the antisymmetric discrete modes. This will demonstrate that the true "finger" pattern is stable. Finally, we heuristically consider the effects of noise, following ideas put forth recently by Bensimon.⁴

Recently, we (together with Koplik⁵) have argued that general mechanisms govern a wide variety of pattern formation problems. We have described this idea as "microscopic solvability" and demonstrated that it explains the workings of simple models of dendritic crystal growth. In Sec. V we review this approach and explain how the re-

sults of this series of two papers lend support to this scenario.

II. PATTERN SELECTION

In the original paper of McLean and Saffman² the allowed value of λ as a function of γ was found by directly solving the steady-state equation. Afterwards, Vanden-Broeck³ reconsidered the same question from a somewhat different point of view. Specifically, he defined a generalized problem via allowing the interface shape to have a cusp at the tip region. This problem then has a solution at all values of λ , with the cusp magnitude $f(\lambda)$ equal to some calculable function of λ at fixed γ . The actual solutions are determined by the auxiliary equation $f(\lambda) = 0$.

For completeness, let us briefly review the formalism in Vanden-Broeck's paper. The steady-state equations can be written as

$$\ln[q(s)] = \frac{-s}{\pi} \int_0^1 \frac{\theta(s')}{s'(s'-s)} ds', \quad (1a)$$

$$\kappa q s \frac{\partial}{\partial s} \left[q s \frac{\partial \theta}{\partial s} \right] - q = -\cos \theta, \quad (1b)$$

with $q(0) = 1$, $q(1) = 0$, $\theta(0) = 0$, and the small parameter κ related to γ via $\kappa = \pi^2 \gamma \lambda / (1 - \lambda)^2$. We fix λ via the condition

$$\ln(1 - \lambda) = \frac{1}{\pi} \int_0^1 \frac{\theta(s')}{s'} ds'$$

and solve the resulting equation with $\theta(1)$ free. The function $f(\lambda)$ is defined to be $\pi/2 - \theta(1)$, which is readily seen, via the relationship

$$x(s) + iy(s) = - \left[\frac{1 - \lambda}{\pi} \right] \int_s^1 ds' \frac{e^{i\theta}}{s' q(s')},$$

to give rise to a nonzero value of $\partial x / \partial y$ at $s = 1$. Since the solution was assumed to be symmetric around $s = 1$ initially, this corresponds to a cusp at the tip.

We have repeated Vanden-Broeck's calculations with identical results. An example of a computed $f(\lambda)$ is shown in Figs. 1(a) and 1(b) for $\gamma = 5 \times 10^{-3}$ and 3×10^{-3} , respectively. (Note that our curves look slightly different because they are plotted at fixed γ , not at fixed κ .) The selected values of λ , $\{\lambda_i\}$, are the zero crossings of f . Of course, this analysis leaves unresolved the question of which of these solutions corresponds to the experimentally observed finger pattern.

The numerical results indicate that as $\gamma \rightarrow 0$, the solutions all approach $\lambda = \frac{1}{2}$. For any $\gamma > 0$, however, all λ_i are strictly greater than $\frac{1}{2}$. It is extremely useful to ask about how $f(\frac{1}{2})$ approaches zero as $\gamma \rightarrow 0$. Our data are plotted in Fig. 2, in the form $\ln f$ versus $1/\sqrt{\gamma}$. This result clearly indicates that

$$f(\frac{1}{2}; \gamma) \sim \exp(-c/\gamma^\alpha), \quad \alpha \cong 0.5. \quad (2)$$

This is a crucial result for all that follows.

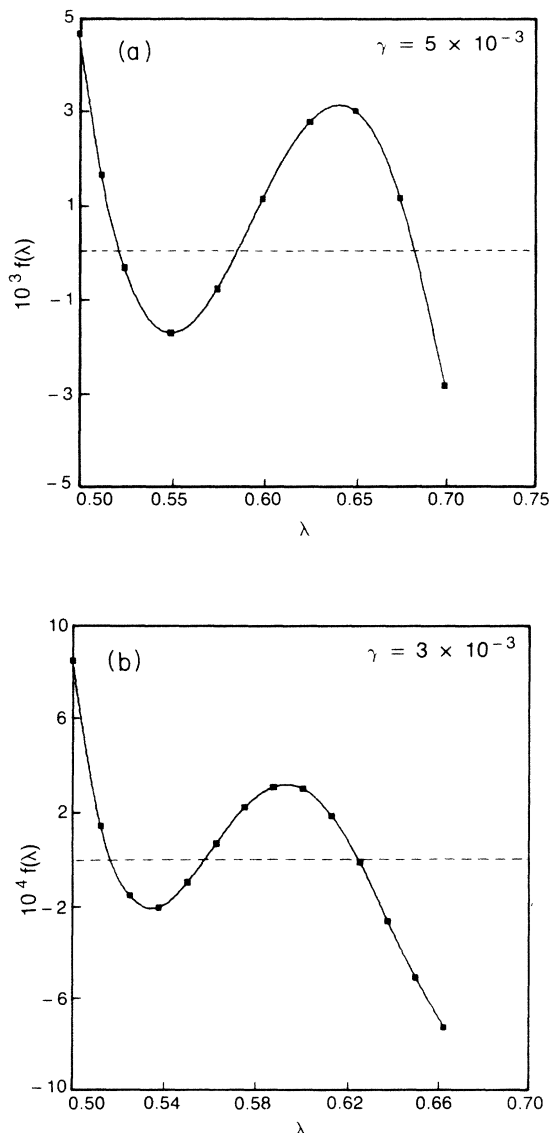


FIG. 1. $f(\lambda)$ vs λ . (a) $\gamma = 5 \times 10^{-3}$, (b) $\gamma = 3 \times 10^{-3}$.

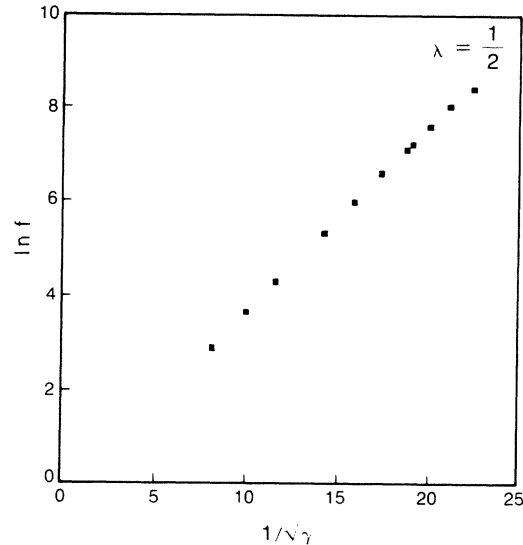


FIG. 2. $\ln[f(\frac{1}{2}; \gamma)]$ vs $1/\sqrt{\gamma}$; exhibition of the essential singularity.

The fact that f has an essential singularity as $\gamma \rightarrow 0$ explains the failure of standard asymptotic analysis. The above formula says that $\lambda = \frac{1}{2}$ is a solution to all orders in an asymptotic expansion around $\gamma = 0$. It is only nonperturbative pieces that spoil the steady-state solution. In other words, we cannot see the solvability condition unless our treatment includes exponentially small terms. We will discuss this idea further in Sec. V.

We now must consider the question of what is the meaning of the stability operator derived via an asymptotic expansion, given that the true solution is determined via exponentially small terms. This will be the subject of Sec. III.

III. SOLVABILITY

So far, we have defined an operator $L(\lambda; \gamma)$ via a steady-state solution which is valid only if we neglect exponentially small terms. Specifically,

$$L(\lambda; \gamma) \equiv \sum_{n=0}^{\infty} L_n(\lambda) \gamma^n, \quad (3)$$

and, in fact, our numerical results have all made use of the truncation of the above series to just two terms. We know, on the other hand, that at an allowed value $\lambda_i(\gamma)$, there exists a true stability operator $\hat{L}(\lambda_i(\gamma), \gamma)$. What is the connection between these two operators? Heuristically, we expect that at all $\lambda \neq \lambda_i$, L has no relationship to any real stability operator. However, at λ_i , $L \cong \hat{L}$. This is because the exponentially small terms which are crucial for $\lambda \neq \lambda_i$ (and in fact prevent that value of the width from actually being a steady-state solution) are either completely absent or totally unimportant at the selected λ . This can be verified by noting that the perturbative steady-state solution agrees extremely well with the numerically computed exact solution.

This idea has immediate consequences. Recall the discussion of the “zero-mode” symmetric discrete eigenvalue at $\lambda = \frac{1}{2}$ as a function of γ . We found that this mode was always at $\text{Re}\omega \leq 0$ even though one could derive in perturbation theory a mode at exactly $\omega = 0$. We can now understand this behavior. At all $\lambda \neq \lambda_i$, the perturbative expansion fails to converge to a true stability operator. Therefore, there is no reason why L should have a mode at $\omega = 0$. Conversely, at $\lambda = \lambda_i$, $L \sim \hat{L}$, which has a zero mode. In other words, only at the selected values of λ should there exist a true translation zero mode.

One can turn around the argument just given to arrive at the following hypothesis: The selected values of λ may be determined by the requirement that L has a translation zero mode. Also, if we have an approximation to L such as $L_0 + \gamma L_1$, we will get approximate values for λ_i . The corrections to these approximate values should go to zero as higher powers of γ . This method is illustrated in Fig. 3, where ω_0 has been plotted versus λ at $\gamma = 0.003$. Notice that ω_0 crosses the axis at $\lambda \sim 0.519$ in excellent agreement (0.5%) with the direct determination as seen in Fig. 1(b). At this relatively low value of γ , it is actually more efficient (less CPU time) to determine λ via this stability criterion than it is to solve the steady-state equation directly.

As discussed above, there is actually a discrete set of λ_i for all γ . To see how this comes about from the point of view of the stability operator, we have studied the lowest three discrete (symmetric) modes at $\gamma = 0.005$, shown in Fig. 4. As before, ω_0 crosses the axis at $\cong 0.524$ in agreement with the results shown in Fig. 1(a) (the agreement is slightly worse at $\gamma = 0.005$ because $L_0 + \gamma L_1$ is a less reliable approximation to L). Note that the next lowest mode, ω_1 , crosses the axis at $\lambda \sim 0.61$. This corresponds to the second zero crossing of $f(\lambda)$ in Fig. 1(b). Eventually, ω_2 will cross, giving rise to a third allowed λ . This

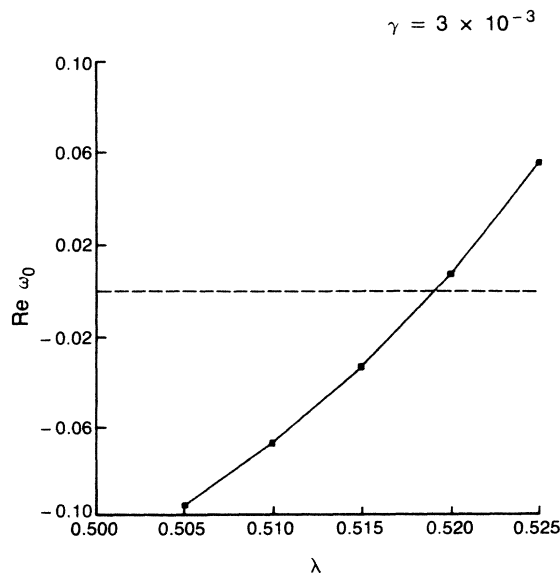


FIG. 3. Lowest symmetric mode ω_0 vs λ at $\gamma = 3 \times 10^{-3}$.

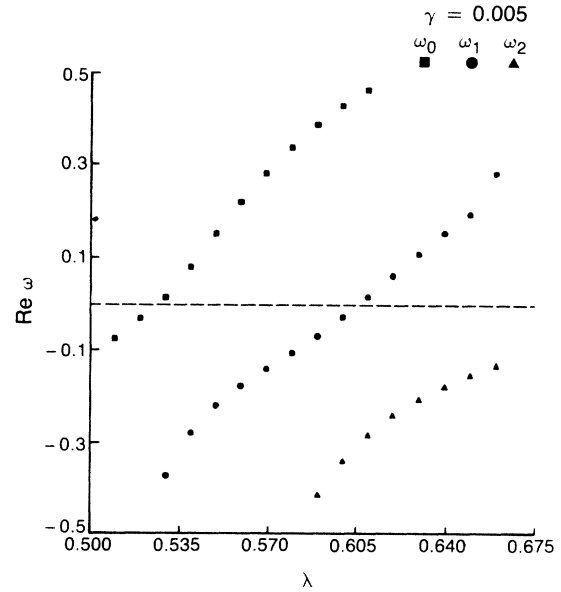


FIG. 4. ω_0, ω_1 , and ω_2 vs λ at $\gamma = 5 \times 10^{-3}$.

behavior persists *ad infinitum*, giving rise to a countably infinite set of allowed finger widths.

We can now suggest a general scenario for the discrete eigenvalues. As we increase λ at fixed γ , or as we decrease γ at fixed $\lambda > \frac{1}{2}$, they all march towards larger $\text{Re}\omega$, eventually crossing the axis. As mentioned in Sec. VI of paper I, more and more discrete modes are generated as γ is lowered, and presumably by the time we reach $\gamma = 0$, an infinite number of modes have crossed the $\text{Re}\omega = 0$ axis. In this sense, the discrete spectrum goes over *continuously* to the exact stability results of Saffman and Taylor⁶ at $\gamma = 0$, i.e., an infinite number of unstable discrete modes. $\lambda = \frac{1}{2}$ is a singular point in this regard, inasmuch as the transition to the $\gamma = 0$ limit does not happen continuously for that value of the width.

This scenario connecting the solvability condition with the stability operator provides a resolution of the question as to why, experimentally, only the smallest $\lambda_i \equiv \lambda^*$ is seen. At any subsequent possible steady-state solution, there is always at least one unstable mode, preventing the steady-state solution from being physically attainable. Given the type of spectrum seen in the figure, this is a *generic* feature of the problem and will not be altered by any small change in the equations or parameters. Because of the fact that higher λ are connected with secondary modes, the instability is inevitable.

There is one feature of this approach that needs clarification. It is perfectly possible to construct a new operator \tilde{L} , which agrees with L to any *fixed* order in γ , which has an exact zero mode. The construction proceeds by recalling that there always exists a function $\delta_N^0(\psi)$, computable in perturbation theory, with

$$L_N[\delta_N^0(\psi)] \equiv \sum_{n=0}^N \gamma^n L_n(\lambda)[\delta_N^0(\psi)] = O(\gamma^{N+1}).$$

Then

$$\tilde{L}_N[\delta] \equiv L_N[\delta] - \delta/\delta_N^0 L_N[\delta_N^0]$$

has δ_N^0 as an exact zero mode. In fact, Bensimon⁴ works with an operator that differs from $L_0 + \gamma L_1$ by terms of order γ^2 and by construction has an exact zero mode. Similarly, the work by Muller-Krumbhaar and Langer⁷ on stability of dendritic crystals employed the above idea to get an exact translation mode. Any physical result, such as the actual spectrum of the finger at the selected λ , will not depend on whether we use L or \tilde{L} —therefore, the instabilities at secondary selected λ_i are still calculable with \tilde{L} . However, results at other λ can be and are different because the operator is not converging to anything. Our use of L is preferable because it allows not only the evaluation of the spectrum at λ_i , but also the determination of λ_i itself.

One should not attach too much physical significance to the fact that the solution is determined by a mode crossing zero. After all, it is *a priori* obvious that any real steady-state solution has an exact translation zero mode. The real physics of the problem lies in the concept of "microscopic solvability," by which we mean the spoiling of allowed steady-state solutions by exponentially small terms in the "microscopic" parameter. The stability method employed here is useful (a) as a computational tool and, more importantly, (b) as it provides an answer to the question of why one can only get a *single* stable steady-state configuration.

Before proceeding to a discussion of the other modes (continuum and/or antisymmetric), we would like to consider the effect that noise might have on our scenario. As we have stressed repeatedly, computations at small numbers of points are always more *unstable* than the true modes, found by extrapolation. Let us suppose that in some sense finite numerical noise in our program acts as a model for physical noise arising from imperfections in the

apparatus. Then, any given experiment would approximately correspond to a numerical analysis at a fixed number of points. In Fig. 5 we exhibit the $N = 50$ values of ω_0 at $\gamma = 0.002$. The curve crosses zero at $\lambda^* = 0.486$, which is then the allowed width. Because of the increased instability, λ^* has been lowered and, in fact, is below the asymptotic limit at zero noise of $\frac{1}{2}$. There have been indications in recent experiments^{8,9} that the width can go below $\frac{1}{2}$ and Bensimon⁴ has independently suggested that this might be due to noise effects. Of course, there are additional three-dimensional considerations present in the experiment that are not accounted for by the system of equations studied here. These effects might also play an important role in resolving this issue.

IV. STABILITY

Now that we have understood how the solvability condition operates, we return to the question which motivated our study, the stability of the finger. In this section, we present results for the continuum, both symmetric and antisymmetric, as well as for antisymmetric discrete modes. The conclusions will be the same as that stated in our earlier paper¹⁰ based on the $\lambda = \frac{1}{2}$ analysis—fingers are stable as far as linear analysis goes. At the end, we briefly discuss the evidence for the nonlinear mechanism whereby real fingers do actually go unstable at finite γ .

In Figs. 6(a) and 6(b) we have shown the extrapolated continuum at $\gamma = 0.005$, $\lambda^* \cong 0.525$, including both the antisymmetric and symmetric modes. As discussed in paper I, there appears to be an antisymmetric branch, a symmetric branch (both of which end at $\text{Im}\omega = 0$, $\text{Re}\omega < 0$), and an extra mode at the bottom of the symmetric continuum. For this set of parameters, at spatial resolution $100\sigma = 2$, this mode is at -0.01 , and it becomes more stable as σ is decreased. The conclusions that can be drawn from these quantitative results, as well as the qualitative study of the continuum at a wide variety of γ , are as follows.

(a) The continuum branches are almost completely unaffected by changing from $\lambda = \frac{1}{2}$ to $\lambda^*(\gamma)$. In all cases, the spectrum lies entirely below $\text{Re}\omega < 0$.

(b) The additional "widening" mode moves much closer to zero, albeit remaining stable. This is to be expected, inasmuch as this mode is only nonzero due to exponentially small terms preventing nearby λ from existing as consistent steady-state solutions.

Again, we cannot present completely accurate extrapolated values because of the need for large s_{max} . As far as the physics is concerned, though, this does not appear crucial inasmuch as these continuum modes play a very small role.

Let us turn to a study of the lowest antisymmetric discrete mode. In Fig. 7 we present data for $\tilde{\omega}_0(\gamma)$, where in each case λ is chosen as $\lambda^*(\gamma)$.¹¹ The results look completely analogous to those seen in Fig. 5 of paper I. At any fixed number of points the mode eventually crosses zero; however, the extrapolated "noiseless" value changes

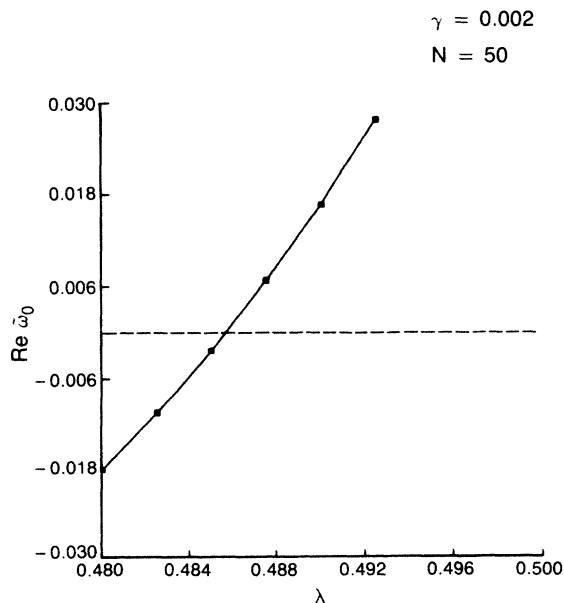


FIG. 5. Noise-induced $\lambda < \frac{1}{2}$; ω_0 vs λ , $\gamma = 0.002$, 50 points.

only slightly and probably does not cross zero until $\gamma=0$. Again, the finger solution is stable to all manner of excitations.

In both real¹² and computer¹³ experiments, there is eventually an antisymmetric instability which destroys the Saffman-Taylor finger. Our studies as well as that of Bensimon suggest that this instability is not a simple bifurcation but instead is subcritical at all $\gamma > 0$. Our results support this idea because of the following observations.

(a) Finite noise leads to instability at $\lambda^*(\gamma)$.

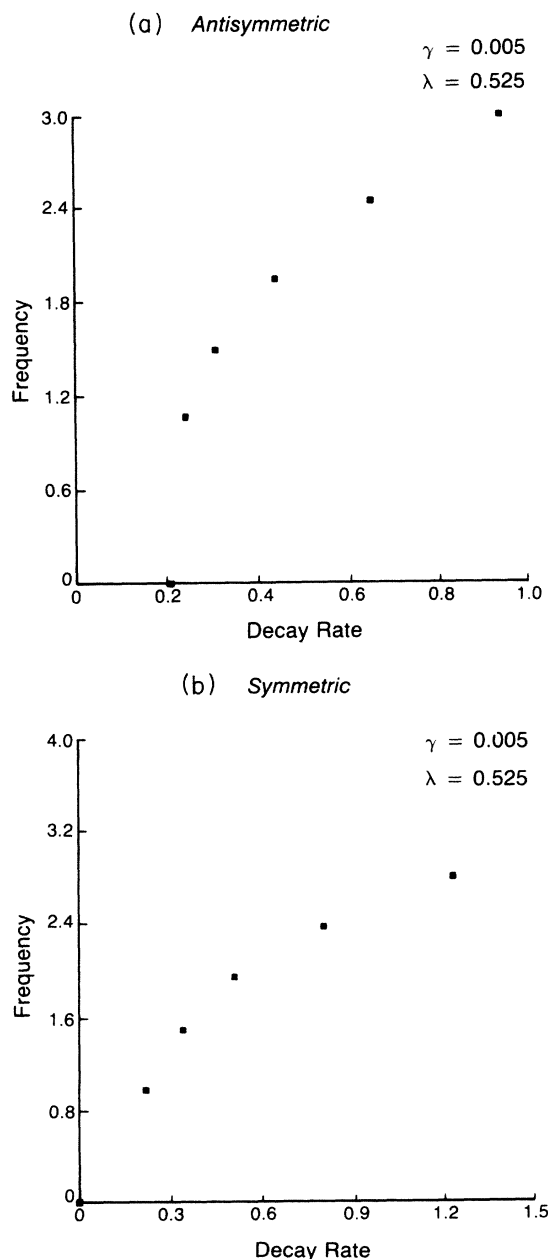


FIG. 6. Continuum modes at $\gamma=5 \times 10^{-3}$. (a) Antisymmetric, (b) symmetric.

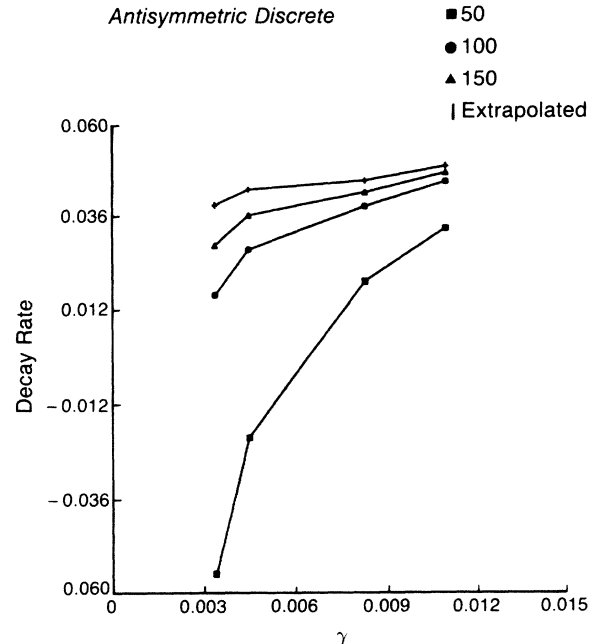


FIG. 7. Lowest antisymmetric mode vs γ .

(b) The stability spectrum becomes a rapidly varying function of λ at small γ —a small change in λ away from λ^* can have a big effect on ω_0 . This suggests that a finite amplitude perturbation, which can effectively change λ and then measure the stability, can act very differently from an infinitesimal perturbation.

(c) The existence experimentally of states below $\lambda = \frac{1}{2}$ attributable to imperfections in the apparatus or to computer resolution can push $\tilde{\omega}_0$ across the $\text{Re}\omega=0$ axis. This can happen because decreasing λ at fixed γ always destabilizes.

Bensimon further suggests that the critical amplitude goes to zero very quickly as $\gamma \rightarrow 0$. Our data seem to confirm this idea, but we have not attempted a quantitative comparison. Any quantitative comparison with real experiments must await further understanding of which features of this transition are universal.

V. CONCLUSIONS

In these two papers, we have presented a phenomenological approach to the selection and stability of the Saffman-Taylor fingers. Along the way, we have analyzed why perturbation theory fails and why simple estimates of the stability can be misleading. More positively, we have shown how to compute the selected width, why the lowest solution is stable, and why all the additional solutions are unstable. What remains, of course, is to find a method of analysis which can predict the features found here and, perhaps most importantly, explain which features are universal and hence will be unchanged when we make the inevitable modifications to the

theory to account for the true experimental situation.¹⁴

In an earlier paper,⁵ the idea of microscopic solvability was introduced as a general means of understanding ordered patterns and their breakdown. The essential component of this idea was the fact that most patterns in diffusively controlled systems were in fact controlled by very small microscopic parameters, usually arising through the microscopic structure of the interface. Included in this is the width of the interface, the capillary length due to surface tension, and, perhaps, the viscous skin depth of a rapidly moving fluid. The reason this can happen is that the growth process is mathematically inconsistent without such a small-scale cutoff. This shows up, for example, as finite time singularities in the interface at $\gamma=0$ for the Hele Shaw system¹⁵ and leads to the importance of carefully considering the effects of finite γ , even if it is extremely small.

This series of two papers has shown that the Saffman-Taylor finger is a very good example of the above situation. This should alleviate the concern expressed by some

researchers¹⁶ that this mechanism for pattern selection is merely an artifact of the simplicity of the model that had been studied to date.^{5,17} Of course, additional effort is needed to see if these ideas will continue to hold for other systems, most notably directional solidification cells and crystal dendrites.

Finally, we comment on what effect the inclusion of corrections to the equations studied here might have. Inasmuch as the essential feature of the problem, namely the restabilization due to surface tension, is present already, any additional modifications will have a small effect. A small effect might, for example, include the shifting of the limiting value of the width as γ goes to zero, and would certainly shift λ^* at finite γ . So, in any regime of the experiments where the two-dimensional version of the equations is not accurate, the value of λ will differ slightly from the results here. One can go on to study these effects now that the fundamental issues of how the system behaves in a unique and stable manner have been clarified.

¹D. Kessler and H. Levine, preceding paper, *Phys. Rev. A* **33**, 2621 (1986).

²J. W. McLean and P. G. Saffman, *J. Fluid Mech.* **102**, 455 (1981).

³J. M. Vanden-Broeck, *Phys. Fluids* **26**, 2033 (1983).

⁴D. Bensimon, *Phys. Rev. A* **33**, 1302 (1986).

⁵D. Kessler, J. Koplik, and H. Levine, in *Conference Proceedings, Meeting of the Electrochemical Society of America, Toronto, 1985* (unpublished), and references therein.

⁶P. G. Saffman and G. I. Taylor, *Proc. R. Soc. London Ser. A* **245**, 312 (1958).

⁷H. Müller-Krumbhaar and J. Langer, *Acta. Metall.* **29**, 145 (1981).

⁸A. Libchaber and P. Tabeling (private communication).

⁹A. DeGregoria and L. Schwartz (private communication).

¹⁰D. Kessler and H. Levine, *Phys. Rev. A* **32**, 1930 (1985).

¹¹A detailed study of $\lambda^*(\gamma)$ for small γ is contained in J. Col-

lins, D. Kessler, and H. Levine (unpublished).

¹²C. W. Park and G. M. Homsy, *Phys. Fluids* **28**, 1583 (1985); A. Libchaber and P. Tabeling (unpublished); E. Ben-Jacob (unpublished); J. Nittman, G. Daccour, and H. E. Stanley, *Nature (London)* **314**, 141 (1985).

¹³A. J. Degregoria and L. Schwartz (unpublished).

¹⁴An example of the corrections that are necessary to account for additional fluid mechanical considerations can be found in C. W. Park and G. M. Homsy, *J. Fluid Mech.* **139**, 291 (1984).

¹⁵D. Bensimon and B. Shraiman, *Phys. Rev. A* **30**, 2840 (1985).

¹⁶W. Van Saarloos and J. D. Weeks, *Phys. Rev. Lett.* **55**, 1685 (1985).

¹⁷E. Ben-Jacob, N. Goldenfeld, J. S. Langer, and G. Schön, *Phys. Rev. Lett.* **51**, 1930 (1983); *Phys. Rev. A* **29**, 330 (1984); E. Ben-Jacob, N. Goldenfeld, G. Kotliar, and J. S. Langer, *Phys. Rev. Lett.* **53**, 2110 (1984).